*Journal of Basic and Applied Research International*

***Volume 30, Issue 5, Page 1-17, 2024; Article no.JOBARI.12300***
***ISSN: 2395-3438 (P), ISSN: 2395-3446 (O)***

# The Performance Evaluation of Aluminum Alloy 356 Cow-Horn Composite as a Turning Machining Material Using Response Surface Methodology

**Bethel Mba [a*], Nwogu Chukwunonso Nweze [a], Uchenna Alozie [b], Franklin Onwuka [c], Clifford Omonini [d] and S. C. Nwoziri [e]**

[a] *Department of Mechanical Engineering, Michael Okpara University of Agriculture, Umudike, Nigeria.*
[b] *Department of Mechanical Engineering, Federal Polytechnic, Nekede, Nigeria.*
[c] *Department of Mechanical Engineering, Federal University of Nigeria, Nsukka, Nigeria.*
[d] *Department of Mechanical and Aerospace Engineering, Nazarbayev University, Astana, Kazakhstan.*
[e] *Department of Mechanical Engineering, University of Calabar, Nigeria.*

***Authors' contributions***

*This work was carried out in collaboration among all authors. All authors read and approved the final manuscript.*

***Article Information***

DOI: https://doi.org/10.56557/jobari/2024/v30i58842

**Open Peer Review History:**
This journal follows the Advanced Open Peer Review policy. Identity of the Reviewers, Editor(s) and additional Reviewers, peer review comments, different versions of the manuscript, comments of the editors, etc are available here: https://prh.ikprress.org/review-history/12300

***Review Article***

***Received: 27/06/2024***
***Accepted: 29/08/2024***
***Published: 04/09/2024***

**Corresponding author: E-mail: mbabethelchidiadi@gmail.com;*

***Cite as:*** *Mba, Bethel, Nwogu Chukwunonso Nweze, Uchenna Alozie, Franklin Onwuka, Clifford Omonini, and S. C. Nwoziri. 2024. "The Performance Evaluation of Aluminum Alloy 356 Cow-Horn Composite As a Turning Machining Material Using Response Surface Methodology". Journal of Basic and Applied Research International 30 (5):1-17. https://doi.org/10.56557/jobari/2024/v30i58842.*

## ABSTRACT

The industry's usage of machining has been restricted by a lack of knowledge and understanding about important input parameters and the machinability of materials, which makes it difficult to fulfill the necessary criteria for material removal rate, surface roughness, tool wear, and many other issues. This paper examines the Performance evaluation of Aluminum alloy 356 cow-horn composite as a turning machining material using response surface methodology. A356/cow horn particles (CHp) composite from Ochieze, 2017, was used as a raw material and the composite composition by mass is 90% Aluminum alloy and 10% cow-horn reinforcement. The molten composite was made more wettable by adding 2% weight of magnesium powder. The addition of magnesium powder reduced the interface energy of the matrix reinforcement and raised the composite's surface energy, which in turn decreased its surface tension. The Response Surface Methodology was utilized to create the experiment's design. After optimization, several significant models are shown with a probability value of less than 0.05. The findings of the analyzed result show that the suggested mathematical models obtained from the data can accurately portray the performance within the limitations of the components under discussion. The investigation demonstrates that, as opposed to depth of cut, cutting speed considerably impacts surface roughness and tool wear rate. Ra and TWR are not significantly affected by the depth of cut. Numerical optimization was used to identify combinations of process parameters that will give the best response. Adjusting the feed rate, depth of cut, and cutting speed to 900 rpm, 0.25 rev/mm, and 1.5 mm achieve the optimal composite turning process at a surface roughness of 160.256 mm, material removal rate of 15.4011 mm3/min, and tool wear of 0.000362687 mg/mm respectively.

*Keywords: Tool wear ratio; aluminum alloy cow horn composites; material removal rate; response surface methodology; surface roughness.*

## 1. INTRODUCTION

Metal matrix composites are gaining popularity in key industries such as aerospace, automotive, and agriculture due to their superior strength, high wear resistance, and elastic modulus compared to low-density materials, Light weight highly contributing to energy consumption. Metal matrix composites are among the best engineering materials because of their numerous valuable attributes, which include outstanding heat stability, stiffness, and conductivity [1-8]. Composite materials are well known for their extraordinary qualities, which include the presence of the matrix phase, a vital component that facilitates load transfer, structural integrity, and improved mechanical properties [9-14]. The composite materials' matrix and reinforcement can be constructed using metal, inorganic, and biological elements. Long and short fibers and particles are the two most common and utilized reinforcing materials [13, 15-19].

Composite materials are preferable to metals in various applications due to their high strength-to-weight ratio, which increases the performance level of diverse engineering applications, high stiffness, and good damage resistance under different operating conditions, thereby significantly advancing engineering to a higher level [20-23]. These unique features make them a desirable substitute for conventional materials in many technological applications to improve optimal performance [11,20,24,25]. A few advantages of composite materials are their increased strength and stiffness, improved fatigue resistance, ability to endure heat, wear, corrosion, and decreased weight [26,27]. Appropriate application-specific properties can be obtained by carefully organizing the metal matrix and adding reinforcement.

Metal Matrix Composites (MMC) are composite materials made from metals such as titanium, magnesium, and aluminum alloys. The reinforced materials, including particles, short (whiskers), or long fibers give composites the stiffness, strength, thermal stability, and other structural properties that improve their performance in their specific application areas [28-31]. Lately, there has been an increase in interest in the development of composites with low-cost, low-density reinforcements to meet engineering goals [32-34].

Aluminum Matrix Composites (AMCs), having aluminum as a principal constituent, are a high-performance, lightweight class of materials [35]. Fibers, whiskers, or particles can serve as low-cost reinforcement in AMCs, with particle materials emerging as the most significant and dominant material [36-38].

One of the most crucial procedures of machining operations in material removal is metal turning [39-41]. Turning mechanism is the most widely used machining method in the industry for creating high-quality components. It is used to create the form and dimensions required for the finishing or semi-finishing of a rotating object. It has determined that developing optimization strategies for choosing cutting conditions in cutting operations quantitative forecasts of various technological performance metrics, ideally equations [42-46]. The critical technical technology for producing multiple mechanical components and products is machining requires optimum selections of best cutting conditions, thereby reducing material waste, time, and tool [47,48]. A standard method of material removal in machining operations is turning. Many academics have investigated the geometrical and material properties of machining. A lack of experience and understanding of material machinability has hampered the use of machining in the industry, thereby increasing the rate at which accidents occur, damaging human beings and machines in use [49-52]. Fabricating numerous mechanical components requires dependable patterns and processes, repeatable processes, and precise instruments [53]. One of the common ways of making desired geometry components is through machining [54]. However, aluminum metal matrix composites (AMMCs) are among the most widely utilized composites because of their ease of fabrication, high strength, and lightweight [55,56]. Disc brake development heavily uses composites in automotive and aerospace engines [57,58]. In the turning operations machining process, the tool's life, the force required for cutting, the roughness of the machined surfaces, and energy consumption are the most crucial cutting performance indicators [54]. The industry's machining utilization has been hindered by a lack of knowledge and understanding regarding the machinability of materials and the crucial input parameters, which makes it difficult to meet the necessary standards for material removal rate, surface roughness, tool wear, and many other factors. The primary issue with turning AMMC is excessive tool wear, which either renders the operation impractical or impossible. Therefore, there are unique requirements for the wear resistance of the cutting tools when machining composite materials. Repeatable procedures, accurate tools, and ideal input variables are needed to fabricate a large number of mechanical parts and the usage of the proper input settings leads to the optimal machining process [59,60].

## 2. MATERIALS AND METHODS

### 2.1 Materials

Materials incorporated into this project include; Aluminum alloy A356, Cow-horn particles and HSS cutting tool, Lathe machine, Surface tester (Surfcorder SE3500) and Dynamometer (XXR-UN01). Figs. 1 and 2 displayed the cow-horn and aluminum alloy 356 samples that were used. The lathe machine configuration for executing a turning operation is shown in Fig. 3.

**Fig. 1. Cow horn**

**Fig. 2. Aluminum alloy 356**

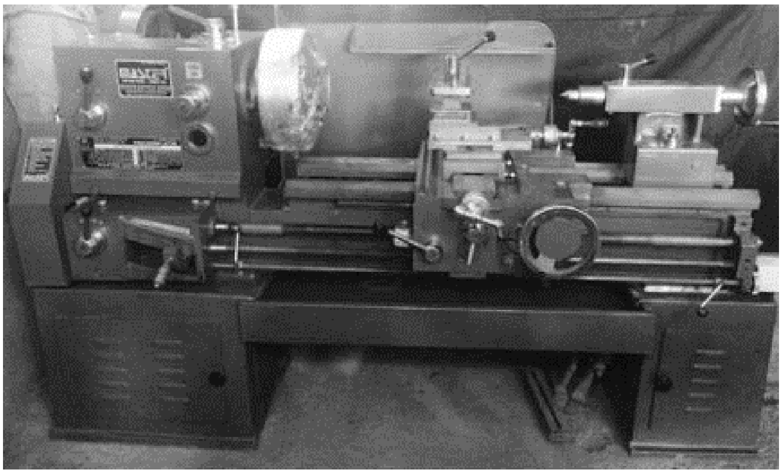

**Fig. 3. Lathe machine setup**

## 2.2 Methods

The cow-horn were collected and cleaned with a blower to remove impurities. Moisture content was removed by heating the cow-horn in an oven at 1150°C [29]. The cow-horn was cooled to room temperature after removing the impurities by heating process. The dried cow horn was processed into a fine powder using a grinding machine [61]. The powder was sieved to obtain the required particles of a uniform size of 150µm [61] which significantly improves the mechanical Properties and enhancement optimal particle distribution. The mold samples were preheated for moisture removal and cooled at room temperature. The composite composition by mass is 90% Aluminum alloy and 10% cow-horn reinforcement [62]. The weights of the reinforcements (cow-horn) were determined using a compact electronic scale. The sourced Aluminum alloy weight for the composite was determined using a weighing balance, and pulverized cow horn was kept in a furnace preheated to improve wettability.

The aluminum alloy was heated to a temperature of 550°C in a crucible furnace powered by diesel, coupled to a temperature probe, and tested to ensure complete melting [62]. To further improve the metal's wettability, magnesium powder (2% weight) was added to the molten metal, and the addition of magnesium powder increased the metal's surface energy, decreasing its surface tension and reducing the interface energy of the matrix reinforcement. The preheated pulverized cow-horn particles were mixed with the liquid aluminum using an automated mechanical stirrer [63]. The composite mixture was super-heated at 550°C [62]. The composite was then created by pouring the combined aluminum alloy cow horn into a mold and letting it cure.

## 3. RESULTS

Response surface methodology (RSM) was used to optimize the turning process of AACHC controlled factors (feed rate, depth of cut and cutting speed) and observed results (surface roughness, material removal rate and tool wear). Optimization was carried out to obtain the best combination level of input variables that gives the best response. Numerical method in RSM was used to find the optimum turning combination of AACHC and its desired response.

The regression model equation was obtained using equation 2. The model selection was based on the effect of the variables (cutting speed, feed rate and depth of cut). The individual response in terms of coded and actual variables is a function of the input variables as related in equation 1.

$$y = f(x_1, x_2, x_3 \dots x_k) \quad (1)$$

$$y = \beta_0 + \beta_1 x_1 + \beta_2 x_2 + \beta_3 x_3 + \beta_{123} x_1 x_2 x_3 + \varepsilon \quad (2)$$

Where;

$x_1 = FR, \;\; x_2 = CS, \; and \;\; x_3 = DC$

y = Required output response (surface roughness, material removal rate and tool wear).

$f$ = Response function

ε = Random error (measurement error on response and background noise)

k is the number of independent variables.

$\beta_0$ is the intercept value of the variables

$\beta_1, \beta_2, \beta_3, \beta_{123}$ are coefficients associated with each variable and interaction of $x_1, x_2, x_3, x_1x_2x_3$ respectively**.**

### 3.1 Machining Operation Using Design of Experiment (DOE)

A preliminary study on A356/cow horn particle composite formulation was done by examining how the machining parameters affect the created material. Three (3) excipients were chosen for A356/cow horn particle formulation based on their function. Two of them and the feed rate were used as variables in the I-optimal custom design as they may affect the responses. The variables' ranges were also studied using the I-optimal custom technique in design expert software. Table 1 shows the summary data table of the actual design after the experiment. Table 2 shows Model terms of build information.

The model terms help to determine the significance of the model and its impact in obtaining optimal result. The power ranges in Table 2 shows the true effect of the model and the power ensures reliability of the result generated.

### 3.2 Surface Roughness

Table 3 shows the interactions and correlations of surface roughness over various input parameters. The surface roughness of the material is influenced positively by the cutting speed and depth of cut, which have a considerable effect; the surface roughness is not affected by feed rate. The material's surface roughness will rise with increased cutting depth and speed. Table 3 shows that model terms affect the cutting conditions when the P-value is less than 0.0500. B and C are essential model terms in this instance. Model terms are unimportant (have no influence) if their values are more extensive than 0.1000.

Table 4 shows the fit statistics for Ra. The table shows that the model added an excellent significant explanation of the data with R2 of 0.9818 and adjusted R2 of 0.8907. The high R2 and adjusted R2 value show that the model explains the data variation instead of being noisy. Obtaining an R-squared of 0.9818, which is in close proximity to 1, indicates that a noteworthy proportion of the data variation is captured by the model. Achieving an adjusted R-squared of 0.8907 suggests that model fit and complexity are well-balanced and also the surface roughness is well explained by input variables. Table 5 evaluates the coefficient in terms of coded factors of Ra.

**Table 1. Summary data table of the actual design after experiment**

| | | | Factor 1 | Factor 2 | Factor 3 | Response 1 | Response 2 | Response 3 |
|---|---|---|---|---|---|---|---|---|
| **Group** | **Run** | | **a: Feed Rate** | **B: Cutting Speed** | **C: Depth of Cut** | **Surface Roughness** | **Material Removal Rate** | **Tool wear** |
| | | | $rev/mm$ | $rpm$ | $mm$ | $mm$ | $mm^3/min$ | $mg/mm$ |
| 1 | AACHC1 | A | 0.15 | 500 | 1 | 121.994 | 24.32 | 0.00074 |
| 1 | AACHC2 | B | 0.15 | 900 | 1.5 | 157.78 | 16.67 | 0.00039 |
| 1 | AACHC3 | C | 0.15 | 900 | 1 | 155.86 | 19.54 | 0.00041 |
| 1 | AACHC4 | D | 0.15 | 500 | 1.5 | 122.211 | 23.34 | 0.00071 |
| 1 | AACHC5 | E | 0.15 | 700 | 0.5 | 124.202 | 22.24 | 0.00065 |
| 2 | AACHC6 | F | 0.15 | 700 | 1 | 127.289 | 20.52 | 0.00063 |
| 2 | AACHC7 | G | 0.15 | 900 | 1.5 | 157.78 | 16.67 | 0.00039 |
| 2 | AACHC8 | H | 0.15 | 700 | 1.5 | 133.484 | 20.29 | 0.00058 |
| 2 | AACHC9 | I | 0.15 | 500 | 0.5 | 119.094 | 30.91 | 0.00092 |
| 2 | AACHC10 | J | 0.15 | 900 | 0.5 | 136.311 | 19.61 | 0.00042 |
| 3 | AACHC11 | K | 0.25 | 900 | 1 | 162.794 | 4.61 | 0.00014 |
| 3 | AACHC12 | L | 0.25 | 900 | 1.5 | 168.47 | 3.75 | 0.00011 |
| 3 | AACHC13 | M | 0.25 | 500 | 0.5 | 131.121 | 15.8 | 0.00037 |
| 3 | AACHC14 | N | 0.25 | 700 | 0.5 | 149.205 | 9.5 | 0.00031 |
| 4 | AACHC15 | O | 0.25 | 900 | 0.5 | 162.194 | 9.31 | 0.00026 |
| 4 | AACHC16 | P | 0.25 | 500 | 1.5 | 158.032 | 12.11 | 0.00034 |
| 4 | AACHC17 | Q | 0.25 | 500 | 1 | 157.88 | 12.5 | 0.00036 |
| 4 | AACHC18 | R | 0.25 | 700 | 1 | 159.992 | 9.48 | 0.0003 |
| 4 | AACHC19 | S | 0.25 | 700 | 1.5 | 161.213 | 7.44 | 0.00028 |

**Table 2. Model terms of build information**

| Term | Standard Error* | Error df† | VIF | Restricted‡ VIF | Power |
|---|---|---|---|---|---|
| A | 0.5515 | 2 | 1.01974 | 1.00356 | 19.1 % |
| B | 0.2890 | 3 | | | 42.2 % |
| B | 0.1704 | 3 | | | |
| C | 0.2930 | 3 | | | 41.1 % |
| C | 0.1688 | 3 | | | |
| Ab | 0.2966 | 3 | | | 42.0 % |
| aB | 0.1694 | 3 | | | |
| Ac | 0.2918 | 3 | | | 39.8 % |
| Ac | 0.1715 | 3 | | | |
| BC | 0.3937 | 3 | | | 16.3 % |
| BC | 0.2457 | 3 | | | |
| BC | 0.2173 | 3 | | | |
| BC | 0.1309 | 3 | | | |

**Table 3. Model terms of surface roughness**

| Source | Term df | Error df | F-value | p-value | |
|---|---|---|---|---|---|
| Whole-plot | 1 | 1.67 | 7.25 | 0.1380 | not significant |
| a-Feed Rate | 1 | 1.67 | 7.25 | 0.1380 | |
| Subplot | 12 | 2.95 | 17.25 | 0.0203 | Significant |
| B-Cutting Speed | 2 | 2.93 | 63.28 | 0.0039 | |
| C-Depth of Cut | 2 | 2.92 | 12.17 | 0.0384 | |
| Ab | 2 | 2.95 | 2.28 | 0.2524 | |
| Ac | 2 | 2.95 | 0.1118 | 0.8978 | |
| BC | 4 | 3.02 | 2.12 | 0.2809 | |

**Table 4. Fit statistics of surface roughness**

| **Std. Dev.** | **9.11** | **$R^2$** | **0.9818** |
|---|---|---|---|
| **Mean** | 145.63 | Adjusted $R^2$ | 0.8907 |
| **C.V. %** | 6.26 | | |

**Table 5. Coefficients in terms of coded factors of surface roughness**

| **Source** | **Coefficient Estimate** | **Standard Error** | **VIF** |
|---|---|---|---|
| Intercept | 144.50 | 4.24 | |
| Whole-plot Terms: | | | |
| a-Feed Rate | 11.42 | 4.24 | 1.00 |
| Subplot Terms: | | | |
| B[1]-Cutting Speed | 12.16 | 1.11 | |
| B[2] | 1.77 | 0.6620 | |
| C[1]-Depth of Cut | 5.43 | 1.14 | |
| C[2] | -1.09 | 0.6433 | |
| aB[1] | -1.87 | 1.18 | |
| aB[2] | -0.9317 | 0.6472 | |
| aC[1] | -0.4497 | 1.14 | |
| aC[2] | 0.2149 | 0.6709 | |
| B[1]C[1] | 3.24 | 1.65 | |
| B[2]C[1] | 2.45 | 1.07 | |
| B[1]C[2] | -0.6823 | 0.8819 | |
| B[2]C[2] | -1.08 | 0.5414 | |

### 3.3 Final Equation in Terms of Coded Factors

$$\textbf{Surface Roughness} = +144.50 + 11.42\mathrm{a} + 12.16\mathrm{B}[1] + 1.77\mathrm{B}[2] + 5.43\mathrm{C}[1] - 1.09\mathrm{C}[2] - 1.87\mathrm{aB}[1] - 0.9317\mathrm{aB}[2] - 0.4497\mathrm{aC}[1] + 0.2149\mathrm{aC}[2] + 3.24\mathrm{B}[1]\mathrm{C}[1] + 2.45\mathrm{B}[2]\mathrm{C}[1] - 0.6823\mathrm{B}[1]\mathrm{C}[2] - 1.08\mathrm{B}[2]\mathrm{C}[2].$$

The Ra response can be predicted using the coded factors equation for specific levels of each factor. The coded equation assists in ascertaining the relative significance of the factors using a comparison of their factor coefficients. The link between the coded factors and the response variable is expressed in the final equation. Engineers can grasp how changes in one or more components affect the result by using this summary of the effects of several factors on surface roughness. The equation can be used to predict the reaction for specific factor sets without the need for additional trials. This predictive power helps with parameter optimization by identifying the optimal combination of variables to get the desired outcome.

### 3.4 Final Equation in Terms of Actual Factors

$$\textbf{Surface Roughness} = 500\mathrm{CS} \times 0.5\mathrm{DC} + 74.29615 + 254.05677\mathrm{FR} \times 500\mathrm{CS} \times 1\mathrm{DC} + 80.71898 + 296.09010\mathrm{FR} \times 500\mathrm{CS} \times 1.5\mathrm{DC} + 82.68288 + 287.19312\mathrm{FR} \times 700\mathrm{CS} \times 0.5\mathrm{DC} + 84.75815 + 259.7267\mathrm{FR} \times 500\mathrm{CS} \times 1\mathrm{DC} + 83.28848 + 301.76010\mathrm{FR} + 700\mathrm{CS} \times 1.5\mathrm{DC} + 88.77588 + 292.86312\mathrm{FR} + 900\mathrm{CS} \times 0.5\mathrm{DC} + 126.18321 + 115.34646\mathrm{FR} + 900\mathrm{CS} \times 1\mathrm{DC} + 127.85104 + 157.37979\mathrm{FR} + 900\mathrm{CS} \times 1.5\mathrm{DC} + 134.12148 + 148.48281\mathrm{FR}$$

For certain levels of each element, the equation expressed in terms of the actual factors predicts the Ra response. Here, each factor's levels should be determined per their original units. Fig. 4 shows the graph of predicted values and actual values of surface roughness.

The fact that the data points are nearly evenly distributed and have few outliers suggests that the data is normally distributed. The predictive model that was employed to estimate surface roughness is validated by the Fig. 4. There is a good model fit as the points are near to the line of perfect agreement.

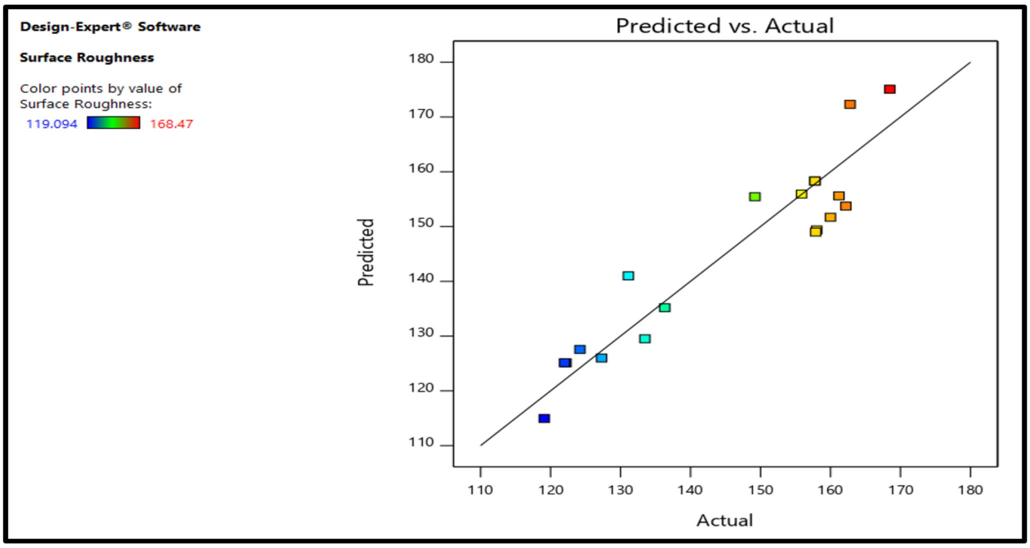


**Fig. 4. Graph of predicted values and actual values of surface roughness**

**Table 6. Model terms of MRR**

| Source | Term df | Error df | F-value | p-value | |
|---|---|---|---|---|---|
| Whole-plot | 1 | 1.25 | 87.20 | 0.0412 | Significant |
| a-Feed Rate | 1 | 1.25 | 87.20 | 0.0412 | |
| Subplot | 12 | 3.00 | 19.15 | 0.0166 | Significant |
| B-Cutting Speed | 2 | 2.83 | 77.05 | 0.0034 | |
| C-Depth of Cut | 2 | 2.81 | 24.80 | 0.0164 | |
| Ab | 2 | 2.88 | 0.2280 | 0.8092 | |
| Ac | 2 | 2.88 | 0.1383 | 0.8763 | |
| BC | 4 | 3.09 | 2.32 | 0.2535 | |

**Table 7. Fit statistics of MRR**

| **Std. Dev.** | **1.62** | **$R^2$** | **0.9932** |
|---|---|---|---|
| **Mean** | 15.72 | Adjusted $R^2$ | 0.9590 |
| **C.V. %** | 10.30 | | |

**Table 8. Coefficients in terms of coded factors of MRR**

| Source | Coefficient Estimate | Standard Error | VIF |
|---|---|---|---|
| Intercept | 15.59 | 0.6787 | |
| Whole-plot Terms: | | | |
| a-Feed Rate | -6.33 | 0.6775 | 1.00 |
| Subplot Terms: | | | |
| B[1]-Cutting Speed | -3.63 | 0.2999 | |
| B[2] | 0.4449 | 0.1796 | |
| C[1]-Depth of Cut | -2.17 | 0.3103 | |
| C[2] | 0.2956 | 0.1732 | |
| aB[1] | 0.2101 | 0.3240 | |
| aB[2] | -0.0311 | 0.1746 | |
| aC[1] | -0.0870 | 0.3109 | |
| aC[2] | 0.0898 | 0.1827 | |
| B[1]C[1] | 0.8588 | 0.4708 | |
| B[2]C[1] | -0.2694 | 0.3105 | |
| B[1]C[2] | -0.5082 | 0.2449 | |
| B[2]C[2] | 0.0658 | 0.1524 | |

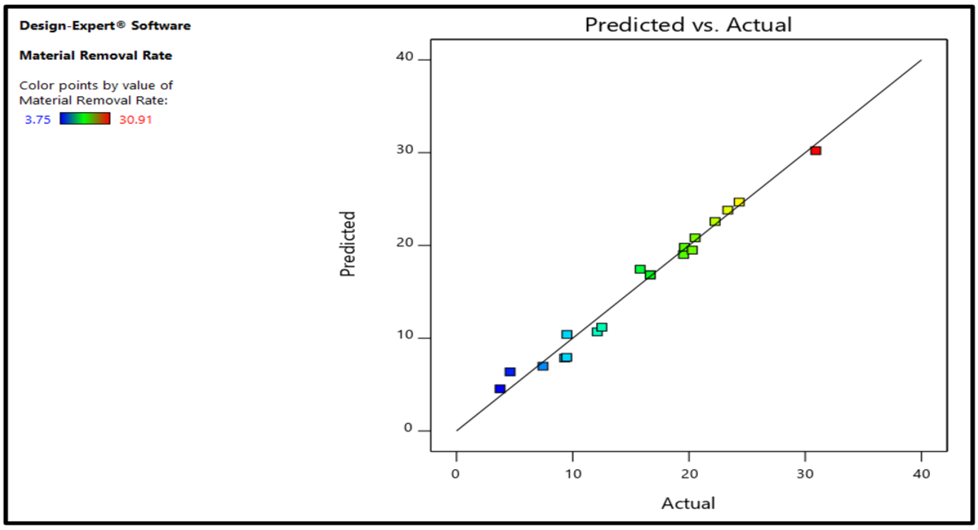


**Fig. 5. Graph of predicted values and actual values of material removal rate**

### 3.5 Material Removal Rate

Table 6 shows that P-values of the essential factors are significant, satisfying the peak performance of the model terms. Model terms A, B, and C are essential in this context. Table 6 displayed the relationships between material removal rate and input parameters. The relevant input parameters that are used have a beneficial impact on the material's MRR. With more input variables, the MRR will increase.

Table 7 shows the fit statistics for MRR. The table shows that the model added an excellent significant explanation of the data with $R^2$ of 0.9932 and adjusted $R^2$ of 0.9590. The high $R^2$ and adjusted $R^2$ value show that the model explains the data variation instead of being noisy. Table 8 evaluates the coefficient in terms of coded factors of MRR.

### 3.6 Final Equation in Terms of Coded Factors

$$\textbf{Material Removal Rate} = +15.59 - 6.33a - 3.63B[1] + 0.4449B[2] - 2.17C[1] + 0.2956C[2] + 0.2101aB[1] - 0.0311aB[2] - 0.0870aC[1] + 0.0898aC[2] + 0.8588B[1]C[1] - 0.2694B[2]C[1] - 0.5082B[1]C[2] + 0.0658B[2]C[2].$$

The MRR reaction can be predicted using the coded factors equation for specific levels of each factor. The link between the coded factors and the response variable is expressed in the final equation. Engineers can grasp how changes in one or more components affect the result by using this summary of the effects of several factors on material removal rate. The result for specific factor sets can be anticipated using the equation without conducting additional experiments. This predictive power helps with parameter optimization by figuring out the best combination of variables to get the desired outcome.

### 3.7 Final Equation in Terms of Actual Factors

$$\textbf{Material Removal Rate} = 500CS \times 0.5DC + 49.10438 - 128.74688FR \times 500CS \times 1DC + 43.91938 - 127.54688FR \times 500CS \times 1.5DC + 42.78625 - 125.30625FR \times 700CS \times 0.5DC + 40.59938 - 123.64687FR \times 700CS \times 1DC + 39.48938 - 122.44687FR \times 700CS + 1.5DC + 37.90625 - 120.20625FR \times 900CS \times 0.5DC + 40.28125 - 129.10625FR \times 900CS \times 1DC + 37.65625 - 127.90625FR \times 900CS \times 1.5DC + 35.40203 - 125.66563FR$$

The equation stating the actual factors predicts the MRR response for specific levels of each factor. In this case, the levels of each factor should be stated in their respective units. Fig. 5 shows the graph of predicted values and actual values of material removal rate.

A normal distribution of the data is suggested by the roughly equal distribution of the data points and the scarcity of outliers. Fig. 5 provides confirmation for the prediction model used to measure material removal rate. Considering that the points are close to the line of perfect agreement, there is a good model fit.

### 3.8 Tool Wear

Table 9 shows that the P-values of the essential factors (A, B, C, and aB) are significant, satisfying the peak performance of the model terms. Table 9 presents the correlation between input parameters and tool wear. A positive effect on tool wear is produced by the pertinent input parameters that are applied. The wear of the tool will rise with more input variables and vice versa.

Table 10 shows the fit statistics for TWR. The table indicates that the model added an excellent significant explanation of the data with $R^2$ of 0.9952 and adjusted $R^2$ of 0.9714. The high $R^2$ and adjusted $R^2$ value show that the model explains the data variation instead of being noisy. Table 11 evaluates the coefficient in terms of coded factors of tool wear.

**Table 9. Model terms of tool wear**

| Source | Term df | Error df | F-value | p-value | |
|---|---|---|---|---|---|
| Whole-plot | 1 | 1.75 | 28.78 | 0.0436 | significant |
| a-Feed Rate | 1 | 1.75 | 28.78 | 0.0436 | |
| Subplot | 12 | 2.95 | 50.42 | 0.0043 | significant |
| B-Cutting Speed | 2 | 2.94 | 185.48 | 0.0008 | |
| C-Depth of Cut | 2 | 2.93 | 25.83 | 0.0137 | |
| Ab | 2 | 2.95 | 32.88 | 0.0096 | |
| Ac | 2 | 2.96 | 0.3995 | 0.7021 | |
| BC | 4 | 3.01 | 3.15 | 0.1858 | |

**Table 10. Fit statistics of tool wear**

| **Std. Dev.** | **0.0001** | **$R^2$** | **0.9952** |
|---|---|---|---|
| **Mean** | 0.0004 | Adjusted $R^2$ | 0.9714 |
| **C.V. %** | 15.17 | | |

**Table 11. Coefficients in terms of coded factors of tool wear**

| Source | Coefficient Estimate | Standard Error | VIF |
|---|---|---|---|
| Intercept | 0.0004 | 0.0000 | |
| Whole-plot Terms: | | | |
| a-Feed Rate | -0.0002 | 0.0000 | 1.00 |
| Subplot Terms: | | | |
| B[1]-Cutting Speed | -0.0001 | 6.991E-06 | |
| B[2] | -4.355E-06 | 4.164E-06 | |
| C[1]-Depth of Cut | -0.0001 | 7.165E-06 | |
| C[2] | 6.591E-06 | 4.055E-06 | |
| aB[1] | 0.0001 | 7.404E-06 | |
| aB[2] | -4.705E-07 | 4.078E-06 | |
| aC[1] | -2.881E-06 | 7.182E-06 | |
| aC[2] | 3.584E-06 | 4.217E-06 | |
| B[1]C[1] | 0.0000 | 0.0000 | |
| B[2]C[1] | 5.986E-06 | 6.682E-06 | |
| B[1]C[2] | -0.0000 | 5.523E-06 | |
| B[2]C[2] | -1.363E-06 | 3.384E-06 | |

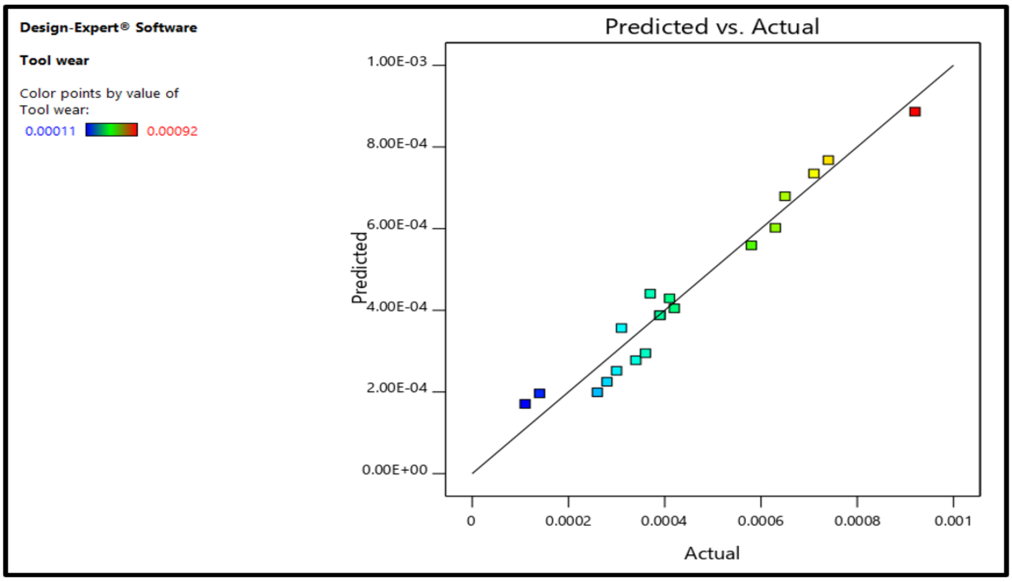


**Fig. 6. Graph of predicted values and actual values of tool wear**

### 3.9 Final Equation in Terms of Coded Factors

$\mathbf{Tool\ Wear} = 0.0004 - 0.0002\mathrm{a} - 0.0001\mathrm{B}[1] - (4.355\mathrm{E} - 06\mathrm{B}[2]) - 0.0001\mathrm{C}[1] + (6.591\mathrm{E} - 0.6\mathrm{C}[2]) + 0.0001\mathrm{aB}[1] - (4.705\mathrm{E} - 07\mathrm{aB}[2]) - (2.881\mathrm{E} - 06\mathrm{aC}[1]) + (3.584 - 06\mathrm{aC}[2]) + 0.0000\mathrm{B}[1]\mathrm{C}[1] + (5.986\mathrm{E} - 06\mathrm{B}[2]\mathrm{C}[1]) - 0.0000\mathrm{B}[1]\mathrm{C}[2] - (1.363\mathrm{E} - 06\mathrm{B}[2]\mathrm{C}[2])$

The reaction can be predicted using the coded factors equation for specific levels of each factor. The relative significance of the factors can be ascertained using the coded TWR equation and factor coefficient comparison. The link between the coded factors and the response variable is expressed in the final equation. Engineers can grasp how changes in one or more components affect the result by using this summary of the effects of several factors on tool wear rate. The equation can be used to anticipate the response for specific factor sets without conducting additional trials. This predictive skill supports parameter optimization by identifying the optimal combination of factors to yield the desired outcome.

### 3.10 Final Equation in Terms of Actual Factors

$\mathbf{Tool\ Wear} = 500\mathrm{CS} \times 0.5\mathrm{DC} + 0.001546 - 0.004504\mathrm{FR} \times 500\mathrm{CS} \times 1\mathrm{DC} + 0.001404 - 0.00427\mathrm{FR} \times 500\mathrm{CS} + 1.5\mathrm{DC} + 0.001370 - 0.004225\mathrm{FR} \times 700\mathrm{CS} \times 0.5\mathrm{DC} + 0.001161 - 0.003404\mathrm{FR} \times 700\mathrm{CS} \times 1\mathrm{DC} + 0.001099 - 0.003171\mathrm{FR} \times 700\mathrm{CS} \times 1.5\mathrm{DC} + 0.001055 - 0.003125\mathrm{FR} \times 900\mathrm{CS} \times 0.5\mathrm{DC} + 0.000858 - 0.002592\mathrm{FR} + 900\mathrm{CS} \times 1\mathrm{DC} + 0.000747 - 0.002358\mathrm{FR} + 900\mathrm{CS} \times 1.5\mathrm{DC} + 0.000721 - 0.002313\mathrm{FR}$

The TWR for specific levels of each ingredient can be examined using the real factors equation. In this instance, the levels of each element should be stated in their original units. Fig. 6 shows the graph of predicted values and actual values of tool wear.

The small number of outliers and the relatively equal distribution of the data points lead to a normal distribution of the data. The prediction model used to calculate the material removal rate is validated in Fig. 6. A good model fit is evident given that the points are near the line of complete agreement.

## 4. OPTIMIZATION USING RSM

The Design-expert software's module for optimization looks for a mix of factor levels that concurrently satisfies all responses and process factors. By choosing the desired outcomes for each element and response, numerical optimization techniques were applied in this work. The AACHCs' numerical optimization procedure was successful at a desirability function of 1. The optimization depicted in Fig. 4 enhances the machining procedure by modifying parameters to accomplish the intended

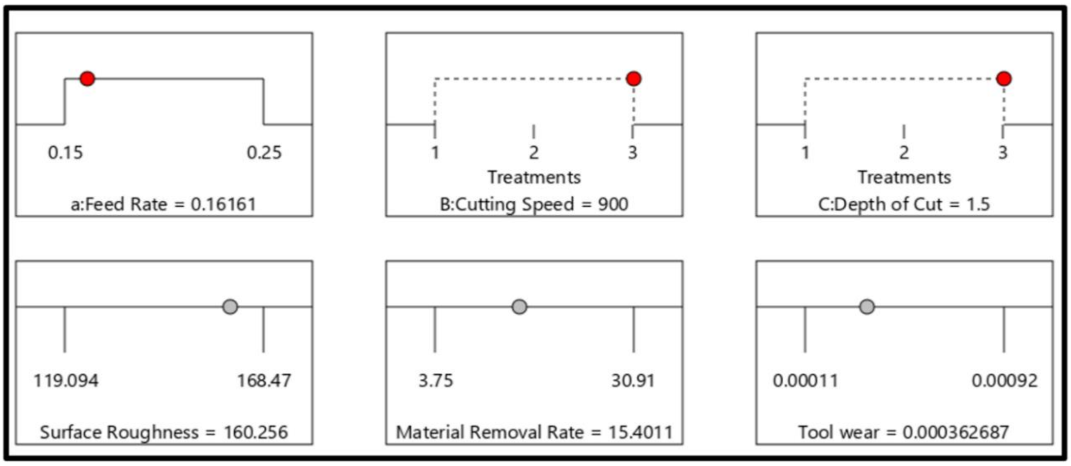


**Fig. 7. Graph of numerical optimization of AACHC**

results, which include reduced tool wear, effective material removal, and a better surface polish. The optimization treatments' outcomes are emphasized by the red dots, which draw attention to particular data points.

Fig. 7 shows the graph of numerical optimization of AACHC. The optimal value was achieved when the feed rate, cutting speed, and depth of cut were at 0.16161 rev/mm, 900 rpm, and 1.5 mm, and it gives the best response at a surface roughness of 160.256 mm, material removal rate of 15.4011 mm3/min, and tool wear of 0.000362687 mg/mm respectively.

## 5. CONCLUSION

This paper examines the optimization of cow horn composite aluminum alloy 356 turning process parameters. The samples were investigated for Ra, MRR after machining with the TWR. From the results of the analyses, the following conclusions are drawn:

1. AACHC, adopted from Ochieze, 2017 was successfully utilized for this investigation.
2. The ANOVA tables of the TWR, Ra, and MRR demonstrate that some models have significant probability values (P-values) less than 0.05.
3. Numerical optimization was used to identify combinations of process parameters and to attain the lowest TWR, MRR, and Ra possible.
4. The impact of process factors on responses was examined individually and in interaction. Cutting speed has an enormous effect on TWR and Ra, as evidence.
5. The TWR and Ra are only a little influenced by the depth of the cut.
6. The regression equation model generated can predict the coded, actual factors' Ra, TWR, and MRR.
7. Adjusting the feed rate, depth of cut, and cutting speed to 900 rpm, 0.25 rev/mm, and 1.5 mm achieve the optimal composite turning process.
8. This research is valuable because it provides information on the optimal input parameters to be used in order to achieve the ideal output parameters. These parameters will minimize material waste, boost energy consumption, and yield the best surface finishing.

## DISCLAIMER (ARTIFICIAL INTELLIGENCE)

Author(s) hereby declares that NO generative AI technologies such as Large Language Models (ChatGPT, COPILOT, etc.) and text-to-image generators have been used during writing or editing of manuscripts.

## COMPETING INTERESTS

Authors have declared that no competing interests exist.

## REFERENCES

1. Yi XS. An Introduction to composite materials. In: Yi XS, Du S, Zhang L. (eds) Composite Materials Engineering. Springer, Singapore. 2018;1.

Available:https://doi.org/10.1007/978-981-10-5696-3_1

2. Chauhan AK, Singh A, Kumar D, Mishra K. Properties of composite materials. In Composite Materials. CRC Press. 2021;61–78.
Available:https://doi.org/10.1201/9781003080633-3

3. Ngo TD. Introduction to composite materials. In composite and nanocomposite materials - from knowledge to industrial applications. Intech Open; 2020.
Available:https://doi.org/10.5772/intechopen.91285.

4. Reduwan Billah SM. Composites and Nanocomposites. 2019;1–67.
Available:https://doi.org/10.1007/978-3-319-92067-2_15-1.

5. Yi XS. An Introduction to composite materials. In composite materials engineering. Springer Singapore. 2018;1:1–61.
Available:https://doi.org/10.1007/978-981-10-5696-3_1.

6. Laghari RA, Jamil M, Laghari AA, Khan AM, Akhtar SS, Mekid S. A critical review on tool wear mechanism and surface integrity aspects of SiCp/Al MMCs during turning: Prospects and challenges. The International Journal of Advanced Manufacturing Technology. 2023;126(7–8):2825–2862.
Available:https://doi.org/10.1007/s00170-023-11178-7.

7. Laghari RA, Li J. Modeling and optimization of cutting forces and effect of turning parameters on SiCp/Al 45% vs SiCp/Al 50% metal matrix composites: A comparative study. SN Applied Sciences. 2021;3(7):706.
Available:https://doi.org/10.1007/s42452-021-04689-z

8. Li J, Laghari RA. A review on machining and optimization of particle-reinforced metal matrix composites. The International Journal of Advanced Manufacturing Technology. 2019;100(9–12):2929–2943.
Available:https://doi.org/10.1007/s00170-018-2837-5

9. Kumar A, Grover N, Manna A, et al. Multi-objective optimization of WEDM of aluminum hybrid composites using AHP and genetic algorithm. Arab J Sci Eng. 2022;47:8031–8043.
Available:https://doi.org/10.1007/s13369-021-05865-4.

10. Hasan KMF, Horváth PG, Alpár T. Potential fabric-reinforced composites: A comprehensive review. Journal of Materials Science. 2021;56(26):14381–14415.
Available:https://doi.org/10.1007/s10853-021-06177-6.

11. Kangishwar S, Radhika N, Sheik AA, Chavali A, Hariharan S. A comprehensive review on polymer matrix composites: Material selection, fabrication, and application. Polymer Bulletin. 2023;80(1):47–87.
Available:https://doi.org/10.1007/s00289-022-04087-4

12. Dawoud MM, Saleh MH. Introductory chapter: Background on composite materials. In characterizations of some composite materials. Intech Open; 2019.
Available:https://doi.org/10.5772/intechopen.80960.

13. Selvam JDR, Dinaharan I, Rai RS. Matrix and reinforcement materials for metal matrix composites. In Encyclopedia of Materials: Composites. Elsevier. 2021;615–639.
Available:https://doi.org/10.1016/B978-0-12-803581-8.11890-9.

14. Singh H, Singh Brar G, Kumar H, Aggarwal V. A review on metal matrix composite for automobile applications. Materials Today: Proceedings. 2021;43:320–325.
Available:https://doi.org/10.1016/j.matpr.2020.11.670.

15. Chairi M, El Bahaoui J, Hanafi I, Mata Cabrera F, Di Bella G. Composite materials: A review of polymer and metal matrix composites, their mechanical characterization, and mechanical properties. In Next Generation Fiber-Reinforced Composites - New Insights. Intech Open; 2023.
Available:https://doi.org/10.5772/intechopen.106624.

16. Egbo MK. A fundamental review on composite materials and some of their applications in biomedical engineering. Journal of King Saud University - Engineering Sciences. 2021;33(8):557–568.
Available:https://doi.org/10.1016/j.jksues.2020.07.007.

17. Dawoud MM, Saleh MH. Introductory chapter: Background on composite materials. In characterizations of some composite materials. Intech Open; 2019. Available:https://doi.org/10.5772/intechopen. 80960.
18. Pramanik S, Cherusseri J, Baban NS, Sowntharya L, Kar KK. Metal matrix composites: Theory, techniques, and applications. In Composite Materials. Springer Berlin Heidelberg. 2017;369–411. https://doi.org/10.1007/978-3-662-49514-8_11.
19. Rajak D, Pagar D, Menezes P, Linul E. Fiber-reinforced polymer composites: Manufacturing, properties, and applications. Polymers. 2019;11(10):1667. Available:https://doi.org/10.3390/polym11101667
20. Alam MA, Ya HH, Sapuan SM, Mamat O, Parveez B, Yusuf M, Masood F, Ilyas RA. Recent advancements in advanced composites for aerospace applications: A review. In advanced composites in aerospace engineering applications. Springer International Publishing. 2022;319–339. Available:https://doi.org/10.1007/978-3-030-88192-4_16.
21. Asyraf MRM, Ilyas RA, Sapuan SM, Harussani MM, Hariz HM, Aiman JM, Baitaba DM, Sanjay MR, Ishak MR, Norkhairunnisa M, Sharma S, Alam MA, Asrofi M. Advanced composite in aerospace applications: Opportunities, challenges, and future perspective. In advanced composites in aerospace engineering applications. Springer International Publishing. 2022;471–498. Avaiable:https://doi.org/10.1007/978-3-030-88192-4_24
22. Parveez B, Kittur MI, Badruddin IA, Kamangar S, Hussien M, Umarfarooq MA. Scientific advancements in composite materials for aircraft applications: A review. Polymers. 2022;14(22):5007. Available:https://doi.org/10.3390/polym14225007
23. Rajak D, Pagar D, Menezes P, Linul E. Fiber-reinforced polymer composites: Manufacturing, properties, and applications. Polymers. 2019;11(10):1667. Available:https://doi.org/10.3390/polym11101667
24. Padhan S, Dash L, Behera SK, Das SR. Modeling and optimization of power consumption for economic analysis, energy-saving carbon footprint analysis, and sustainability assessment in finish hard turning under graphene nanoparticle–assisted minimum quantity lubrication. Process Integration and Optimization for Sustainability. 2020;4:445-463. Available:https://doi.org/10.1007/s41660-020-00132-9.
25. Yi XS. An introduction to composite materials. In Composite Materials Engineering,. Springer Singapore. 2018;1:1–61. Available:https://doi.org/10.1007/978-981-10-5696-3_1
26. Ic YT, Saraloğlu Güler E, Sezer B, et al. Multi-objective optimization of turning parameters for SiC- or Al2O3-Reinforced Aluminum Matrix Composites. Process Integr Optim Sustain. 2021;5:609–623. Available:https://doi.org/10.1007/s41660-021-00169-4
27. Butola R, Sharma V, Kanwar S, et al. Optimizing the machining variables in CNC turning of aluminum-based hybrid metal matrix composites. SN Appl. Sci. 2020;2:1356. Available:https://doi.org/10.1007/s42452-020-3155-8.
28. Geng L, Wu K. Metal Matrix Composites. In: Yi XS, Du S, Zhang L. (eds) Composite Materials Engineering. Springer, Singapore. 2018;2. Available:https://doi.org/10.1007/978-981-10-5690-1_3
29. Ahamed S, Roshan JD, Shilpa PC. A literature review on aluminium-7075 metal matrix composites. International Research Journal of Engineering and Technology. 2019;6(6):1384-1390.
30. Hasan KMF, Horváth PG, Alpár T. Potential fabric-reinforced composites: A comprehensive review. Journal of Materials Science. 2021;56(26):14381–14415. Available:https://doi.org/10.1007/s10853-021-06177-6
31. Parveez B, Kittur MI, Badruddin IA, Kamangar S, Hussien M, Umarfarooq MA. Scientific advancements in composite materials for aircraft applications: A review. Polymers. 2022;14(22):5007.

Available:https://doi.org/10.3390/polym14225007.

32. Abdur Rahman M, Haque S, Athikesavan MM, Kamaludeen MB. A review of environmentally friendly green composites: Production methods, current progresses, and challenges. Environmental Science and Pollution Research. 2023;30(7):16905–16929.
Available:https://doi.org/10.1007/s11356-022-24879-5.

33. Crupi V, Epasto G, Napolitano F, Palomba G, Papa I, Russo P. Green composites for maritime engineering: A review. Journal of Marine Science and Engineering. 2023;11(3):599.
Available:https://doi.org/10.3390/jmse11030599.

34. Yang L, Park D, Qin Z. Material function of mycelium-based bio-composite: A review. Frontiers in Materials. 2021;8.
Available:https://doi.org/10.3389/fmats.2021.737377.

35. Srinivasan V, Kunjiappan S, Palanisamy P. A brief review of carbon nanotube reinforced metal matrix composites for aerospace and defense applications. International Nano Letters. 2021;11(4):321–345.
Available:https://doi.org/10.1007/s40089-021-00328-y.

36. Barot RP, Desai RP, Sutaria MP. Recycling of Aluminium Matrix Composites (AMCs): A Review and the Way Forward. International Journal of Metal casting. 2023;17(3):1899–1916.
Available:https://doi.org/10.1007/s40962-022-00905-7.

37. Mistry JM, Gohil PP. Research review of diversified reinforcement on aluminum metal matrix composites: Fabrication processes and mechanical characterization. Science and Engineering of Composite Materials. 2018;25(4):633–647.
Available:https://doi.org/10.1515/secm-2016-0278.

38. Su J, Teng J. Recent progress in graphene-reinforced aluminum matrix composites. Frontiers of Materials Science. 2021;15(1):79– 97.
Available:https://doi.org/10.1007/s11706-021-0541-0.

39. Omietimi H, Afolalu SA, Kayode JF, Monye SI, Lawal SL, Emetere ME. An overview of material removal processes and its importance. E3S Web of Conferences. 2023;391:01077.
Available:https://doi.org/10.1051/e3sconf/202339101077.

40. Stephenson DA, Agapiou JS. Metal Cutting Theory and Practice. CRC Press; 2018.
Available:https://doi.org/10.1201/9781315373119.

41. Valaki J. Experimental study on feasibility of a novel vegetable oil-based pressurized spray cooling system for sustainable surface grinding process. In Sustainable Manufacturing. Elsevier. 2021;61–86.
Available:https://doi.org/10.1016/B978-0-12-818115-7.00005-5.

42. Chen X, Li C, Tang Y, Li L, Li H. Energy efficient cutting parameter optimization. Frontiers of Mechanical Engineering. 2021;16(2):221–248.
Available:https://doi.org/10.1007/s11465-020-0627-x

43. Li B, Tian X, Zhang M. Modeling and multi-objective optimization of cutting parameters in the high-speed milling using RSM and improved TLBO algorithm. The International Journal of Advanced Manufacturing Technology. 2020;111(7–8):2323–2335.
Available:https://doi.org/10.1007/s00170-020-06284-9.

44. Tefera AG, Sinha DK, Gupta G. Experimental investigation and optimization of cutting parameters during dry turning process of copper alloy. Journal of Engineering and Applied Science. 2023;70(1):145.
Available:https://doi.org/10.1186/s44147-023-00314-5

45. Trifunović M, Madić M, Marinković D, Marinković V. Cutting parameters optimization for minimal total operation time in turning pom-c cylindrical stocks into parts with continuous profile using a PCD Cutting Tool. Metals. 2023;13(2):359.
Available:https://doi.org/10.3390/met13020359

46. Wang J. Intelligent Optimization of Cutting Parameters. 2024;25–65.
Available:https://doi.org/10.1007/978-981-99-2011-2_2

47. Wen X, Liu J, Du C, Qu P, Sheng S, Liu X, Zhou H, Kang C, Chen Y, Dong L. The key technologies of machining process design: A review. The International Journal of Advanced Manufacturing Technology. 2022;120(5–6):2903–2921.
Available:https://doi.org/10.1007/s00170-022-08982-y.

48. Zhu K. Introduction to the smart machining system. 2022;1–18.
Available:https://doi.org/10.1007/978-3-030-87878-8_1

49. Finn ME, Tartaglia JM. Prevention of machining-related failures. Journal of Failure Analysis and Prevention. 2022;22(1):191–202.
Available:https://doi.org/10.1007/s11668-021-01329-x.

50. Jamil M, He N, Wei Z, Mushtaq RT, Khan AM, Hegab H, Gupta MK, Khanna N. A state-of-the-art review on sustainability evaluation of machining processes involving the effects of advanced cooling technologies. The International Journal of Advanced Manufacturing Technology. 2024;131(9–10):4377–4402.
Available:https://doi.org/10.1007/s00170-024-13303-6.

51. Pimenov DY, Kiran M, Khanna N, Pintaude G, Vasco MC, Da Silva LRR, Giasin K. Review of improvement of machinability and surface integrity in machining on aluminum alloys. The International Journal of Advanced Manufacturing Technology. 2023;129(11–12):4743–4779.
Available:https://doi.org/10.1007/s00170-023-12630-4.

52. Rance J, Hall S, De Bartolomeis A, Shokrani A. Future Direction of the Sustainable Turning of Difficult-to-Machine Materials. 2019;111–120.
Available:https://doi.org/10.1007/978-981-13-9271-9_11

53. Finn ME, Tartaglia JM. Prevention of machining-related failures. Journal of Failure Analysis and Prevention. 2022;22(1):191–202.
Available:https://doi.org/10.1007/s11668-021-01329-x

54. Selvakumara S, Ravikumar R. Experimental analysis and mathematical modeling of optimized cutting parameters in micro turning. Indian Journal of Engineering and Materials Sciences. 2014;21:397-408.

55. Ayar MS, George PM, Patel RR. Advanced research progresses in Aluminium metal matrix composites: An overview. 2021;020026.
Available:https://doi.org/10.1063/5.0036141

56. Vasava AS, Singh D. A Review on the Manufacturing of Aluminum Metal Matrix Composite by Various Stir Casting Method. 2021;341–349.
Available:https://doi.org/10.1007/978-981-16-3033-0_32.

57. Biswas P, Mondal MK. Evaluation of a Cast Al-Mg2Si Composite for automobile disk-brake rotor application. Journal of Materials Engineering and Performance; 2023.
Available:https://doi.org/10.1007/s11665-023-08760-1.

58. Singh M, Garg HK, Maharana S, Muniappan A, Loganathan MK, Nguyen TVT, Vijayan V. Design and analysis of an automobile disc brake rotor by using hybrid Aluminium Metal Matrix Composite for High Reliability. Journal of Composites Science. 2023;7(6):244.
Available:https://doi.org/10.3390/jcs7060244.

59. Singh A, Kelkar N, Natarajan K, Selvaraj S. Review on the extraction of calcium supplements from eggshells to combat waste generation and chronic calcium deficiency. Environmental Science and Pollution Research. 2021;28(34):46985–46998.
Available:https://doi.org/10.1007/s11356-021-15158-w

60. Kui GWA, Islam S, Reddy MM, Khandoker N, Chen VLC. Recent progress and evolution of coolant usages in conventional machining methods: A comprehensive review. The International Journal of Advanced Manufacturing Technology. 2022;119(1–2):3–40.
Available:https://doi.org/10.1007/s00170-021-08182-0.

61. Prasad SK, Krishna RA. Production and mechanical properties of A356.2/RHA composites. International Journal of Advanced Science and Technology. 2011;33:51–58.

62. Ochieze BQ, Nwobi-Okoye CC, Atamuo PN. Experimental study of the effect of wear parameters on the wear behavior of A356 alloy/cow Horn Particulate

Composites. Journal of Elsevier. 2017;14(1):77-81.
Available:https://doi.org/10.1016/j.dt.2017.11.001.

63. Nwobi-Okoye CC, Uzochukwu CU. RSM and ANN modeling for production of Al 6351/ Egg Shell Reinforced Composite: Multi objective optimization using genetic algorithm. 2019;PII:S2352-4928(19)30689-0.
Available:https://doi.org/10.1016/j.mtcomm.2019.100674



*Peer-review history:*
*The peer review history for this paper can be accessed here:*
*https://prh.ikprress.org/review-history/12300*